JOURNAL OF GUIDANCE, CONTROL, AND DYNAMICS
Vol. 32, No. 5, September–October 2009

Roll–Pitch–Yaw Integrated Robust Autopilot Design for a High Angle-of-Attack Missile

Seonhyeok Kang* and H. Jin Kim†
Seoul National University, Seoul 151-742, Republic of Korea
Jin-Ik Lee‡ and Byung-Eul Jun‡
Agency for Defense Development, Daejeon 305-600, Republic of Korea
and
Min-Jea Tahk§
Korea Advanced Institute of Science and Technology, Daejeon 305-701, Republic of Korea

DOI: 10.2514/1.39812

This paper explores the feasibility of roll–pitch–yaw integrated autopilots for a high angle-of-attack missile. Investigation of the aerodynamic characteristics indicates strong cross-coupling effects between the motions in longitudinal and lateral directions. Robust control techniques based on H_∞ synthesis are employed to design roll–pitch–yaw integrated autopilots. The performance of the proposed roll–pitch–yaw integrated controller is tested in high-fidelity nonlinear 5-degree-of-freedom simulations. The proposed controllers are scheduled as a function of total angle of attack in a linear parameter varying framework with proportional navigation guidance laws. The integrated controller demonstrates satisfactory performance that cannot be achieved by the controller designed in a decoupled manner.

Nomenclature

a_z, a_y	=	normal and lateral acceleration
$C_x \cdots C_{n_r}$	=	aerodynamic coefficients
D	=	reference diameter
F_x, F_y, F_z	=	aerodynamic forces
I_{xx}, I_{yy}, I_{zz}	=	moments of inertia
M	=	Mach number
M_x, M_y, M_z	=	aerodynamic moments
m	=	missile mass
Q	=	dynamic pressure
S	=	reference area
p, q, r	=	roll, pitch, and yaw rates
u, v, w	=	velocity components along the body axes
α	=	angle of attack
β	=	sideslip angle
$\delta_{r,z,y}$	=	roll, pitch, and yaw fin deflections
ϕ, θ, ψ	=	Euler angles

I. Introduction

CLASSICAL approaches, which ignore cross-coupling effects by considering each of the roll, pitch, and yaw axes independently, have dominated the tactical missile autopilot design over the past several decades. For instance, separate proportional and integral controllers are designed for the roll, pitch, and yaw axes at a variety of linearized conditions and were scheduled by appropriate algorithms to account for the change of operating points [1]. If the interaction between each channel is minimal, this three-loop approach for missile autopilots is adequate. However, as the angle of attack increases, for instance, the cross-coupling effects increase which may result in unpredictable performances.

Since the 1980s, development of robust control theory has introduced techniques such as H_∞ and μ synthesis which have been used to design multivariable controllers [2]. These multivariable robust control techniques are particularly beneficial for missile control applications. They allow the formulation of the robustness and performance requirements with respect to plant uncertainty or disturbance, and the numerical computation of a controller design problem in a multi-input/multi-output setting. The resulting controller can cover a wider flight envelope and offer systematic treatment of the fully coupled missile dynamics.

However, the robust control techniques are often less intuitive than the classical techniques, and there have been only a few reports on the roll–pitch–yaw integrated autopilot design using robust control theory. A gain-scheduled autopilot for a bank-to-turn (BTT) missile is designed by the H_∞ loop-shaping approach, to control normal acceleration and bank angle while maintaining the lateral acceleration to zero [3]. H_∞ control is applied to BTT missile autopilot design, in combination with neural networks to compensate partially unknown dynamics [4]. μ synthesis is employed to design separate yaw and roll controllers for a skid-to-turn (STT) missile. Then the performance of the proposed robust controller is demonstrated against nonlinear dynamics [5]. In case of aircraft, a velocity tracking controller for a rotorcraft unmanned aerial vehicle (UAV) is designed by H_∞ control using the fully coupled dynamics [6]. Separate inner and outer loop controllers are employed to complete a UAV mission. Dynamic inversion has been used as the inner loop, and H_∞ control is used as the outer loop, to achieve robust performance [7].

Although linear robust control techniques are capable of covering a significant fraction of the flight envelope, it is likely that a single controller will not suffice to satisfy all performance and robustness requirements throughout the full envelope, especially for agile missiles with rapidly changing nonlinear dynamics. One way to circumvent this difficulty is a linear parameter varying (LPV) controller taking account of the dependence of missile dynamics on the time varying parameters [8]. LPV models of aircraft have been developed using various approaches, such as Jacobian linearization, state transformation, and function substitution [9]. A linear matrix inequality-based controller has also been designed [10]. For a bank-to-turn missile, a loop-shaping approach [3] has been employed to control the longitudinal acceleration and roll angle. For an STT

Received 16 July 2008; revision received 29 May 2009; accepted for publication 16 June 2009.

*Graduate Student, School of Mechanical and Aerospace Engineering.
†Associate Professor, School of Mechanical and Aerospace Engineering.
‡Researcher, Guidance and Control Directorate.
§Professor, Department of Aerospace Engineering.

missile, the μ controllers have been scheduled as a function of dynamic pressure [5]. However, the previous works that employed these robust control techniques have been usually limited to simplified or decoupled missile dynamics, or applied to longitudinal [8] or lateral axis [5] only, rather than the roll–pitch–yaw dynamics with coupling phenomena.

In this research, an H_∞ LPV controller is designed for a 5-degree-of-freedom (DOF) model of a STT missile, which is obtained by fixing longitudinal velocity in a full 6-DOF nonlinear dynamics. An investigation of the aerodynamic characteristics of the missile justifies the necessity of the combined longitudinal/lateral design for high angle-of-attack missiles. A high-fidelity 5-DOF nonlinear simulation accounting for cross-coupling effects between each channel is used to verify the performance and robustness of the proposed controllers. Furthermore, scheduling of the proposed H_∞ controllers is performed for a three-dimensional pursuit scenario, which supports the applicability of the designed autopilot over a wide envelope.

Section II describes the 5-DOF model of a surface-to-air missile used in this research. In Sec. III, we analyze the aerodynamic characteristics to observe cross-coupling effects caused by simultaneous pitch and yaw maneuvering. In Sec. IV, an H_∞ control design problem is formulated for the missile autopilots, followed by a description of the LPV framework. Section V presents the performance of these controllers using high-fidelity nonlinear 5-DOF simulations. Also, LPV controllers are tested in a three-dimensional engagement scenario to check the full-envelope control capability. Section VI summarizes this paper.

II. Missile Model

We begin with the equations of motion for a missile with an axisymmetric configuration in the body coordinate frame. It is assumed that the missile performs a gliding maneuver after the combustion period, so the longitudinal velocity u is constant. This is reasonable because 1) the longitudinal velocity u of propulsion-gliding solid propellant missiles is uncontrollable and changes slowly after the combustion period, and 2) the existing characteristics of the missile, such as nonlinearity and cross-coupling effects among each axis, could be mostly maintained [11].

The force and moments equations are

$$\begin{aligned}\dot{u} &= vr - wq - g\sin\theta + F_x/m\\ \dot{v} &= wp - ur + g\sin\phi\cos\theta + F_y/m\\ \dot{w} &= uq - vp + g\cos\phi\cos\theta + F_z/m\end{aligned} \tag{1}$$

$$\begin{aligned}\dot{p} = M_x/I_{zz} \qquad \dot{q} &= \{(I_{zz} - I_{xx})pr + M_y\}/I_{yy}\\ \dot{r} &= \{(I_{xx} - I_{yy})pq + M_z\}/I_{zz}\end{aligned} \tag{2}$$

where (u, v, w) are the velocity components and (p, q, r) the corresponding angular rates. (F_x, F_y, F_z) represent the aerodynamic forces, (M_x, M_y, M_z) the aerodynamic moments, (ϕ, θ, ψ) the Euler angles, (I_{xx}, I_{yy}, I_{zz}) the moment of inertia, and m the missile mass.

The aerodynamic forces and moments are determined by

$$F_x = -QS(C_x + C_{x_b}) + ma_T \quad F_y = QSC_y \quad F_z = QSC_z \tag{3}$$

$$\begin{aligned}M_x &= QSD\{C_l + (D/2V_m)C_{l_p}p\}\\ M_y &= QSD\{C_m + (D/2V_m)C_{m_q}q\}\\ M_z &= QSD\{C_n + (D/2V_m)C_{n_r}r\}\end{aligned} \tag{4}$$

where Q is the dynamic pressure, S the reference area, D the diameter, a_T the thrust, and V_m the total velocity of the missile. The aerodynamic coefficients, $C_x, \ldots, C_{n_r}$ are extracted from an aerodynamic module that takes into account the current values of altitude, Mach number M, angle-of-attack α, sideslip angle β, and fin deflection angle δ.

III. Model Analysis

The aerodynamic coefficients are extracted from an aerodynamic module based on an experimental database according to altitude, Mach number M, angle-of-attack α, sideslip angle β, and control deflection angle δ, and used to calculate total forces and moments.

The asymmetric airflow on control surfaces for a cruciform tail-controlled missile can generate induced roll moments, which bring about control difficulties, unless the angle of attack equals the sideslip angle. It is difficult to accurately estimate the induced roll moment for which the extent is greatly affected by the angle of attack, Mach number, and fin configurations. When the control inputs are zero, the variation of the roll moment coefficient appears to be a trigonometrical function with the period of 90 deg in Fig. 1a, showing the peak values at $\phi = 22.5$ and 67.5 deg. This corresponds to roughly 15% of the total roll moments generated by roll control inputs. The smaller the Mach number is, the larger the peak value becomes. Accordingly, not only can the consequence of these effects deteriorate the performance of missiles, but they can give rise to unexpected dynamic characteristics. Figure 1b shows the induced roll moment coefficient as α varies from 0 to 20 deg, with a constant bank angle at 0, 5, 10, and 20 deg. It can be seen that the coefficient C_l is large in the low Mach number and large sideslip angle region.

The effects of roll control inputs on the missile model are shown in Figs. 1c and 1d. Figure 1c shows the plots of C_l versus roll control δ_r at each value of sideslip angle and Mach number, when $\alpha = 0$ deg. Figure 1d shows the similar plots when $\alpha = 20$ deg. It should be noted that the roll moments can be generated without roll control inputs when the angle-of-attack α is nonzero. Especially, when the missile maneuvers in the low Mach number and high angle-of-attack region, this phenomenon is noticeable. These cross-coupling effects caused by simultaneous pitch and yaw maneuvering make the control problem more difficult, and our objective is to design a controller that can formally address this issue so that the guidance commands tracking performance are improved.

IV. Controller Design

This section addresses the problem formulation for an integrated roll–pitch–yaw autopilot and LPV framework.

A. Linearization of the Nonlinear Missile Dynamics

The H_∞ synthesis of the missile autopilot system begins with the linearization of the nonlinear missile dynamics of Eqs. (1) and (2). Then we arrive at the following linearized 5-DOF model :

$$\begin{bmatrix}\dot{w}\\ \dot{q}\\ \dot{v}\\ \dot{p}\\ \dot{r}\end{bmatrix} = \begin{bmatrix}Z_w & Z_q & Z_v & Z_p & 0\\ M_w & M_q & M_v & M_p & 0\\ Y_w & 0 & Y_v & Y_p & Y_r\\ L_w & 0 & L_v & L_p & 0\\ N_w & 0 & N_v & N_p & N_r\end{bmatrix}\begin{bmatrix}w\\ q\\ v\\ p\\ r\end{bmatrix} + \begin{bmatrix}Z_{\delta_z} & 0 & 0\\ M_{\delta_z} & 0 & 0\\ 0 & 0 & Y_{\delta_y}\\ L_{\delta_z} & L_{\delta_r} & L_{\delta_y}\\ 0 & 0 & N_{\delta_y}\end{bmatrix}\begin{bmatrix}\delta_z\\ \delta_r\\ \delta_y\end{bmatrix} \tag{5}$$

It is assumed that all state variables are measurable. From Eq. (5), the longitudinal and lateral accelerations are given by $a_z = z_w(\mathbf{x})w + z_v(\mathbf{x})v + z_{\delta_z}(\mathbf{x})\delta_z$ and $a_y = y_w(\mathbf{x})w + y_v(\mathbf{x})v + y_{\delta_y}(\mathbf{x})\delta_y$, respectively, where $\mathbf{x} = [\,w \quad q \quad v \quad p \quad r\,]^T$ is the state vector.

Because of the largest value of L_{δ_r}, which is about 100 times larger than other coefficients in Eq. (5), even the small aileron deflections can greatly affect the roll-rate p that leads to a change of motions in pitch and yaw channels represented by M_p and N_p, respectively. Furthermore, if we ignore these cross-coupling effects, the equations

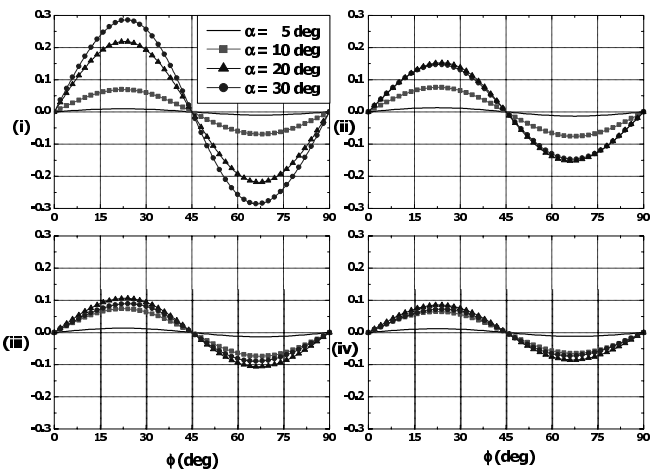

a) C_l versus ϕ

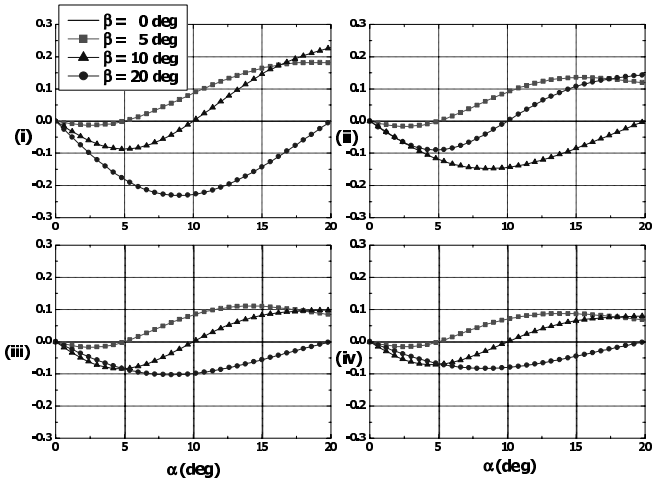

b) C_l versus α

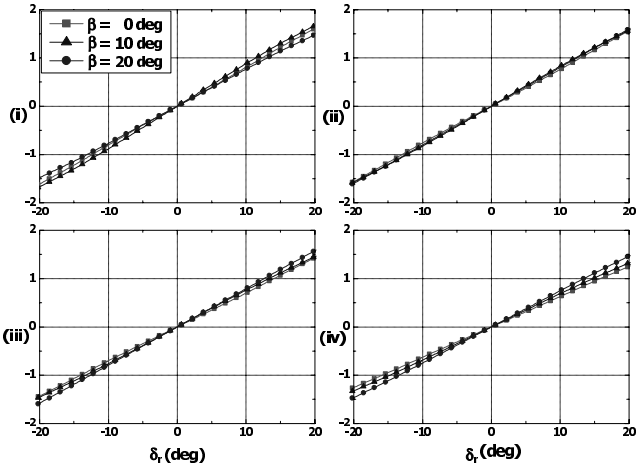

c) C_l versus δ_r with α = 0 deg

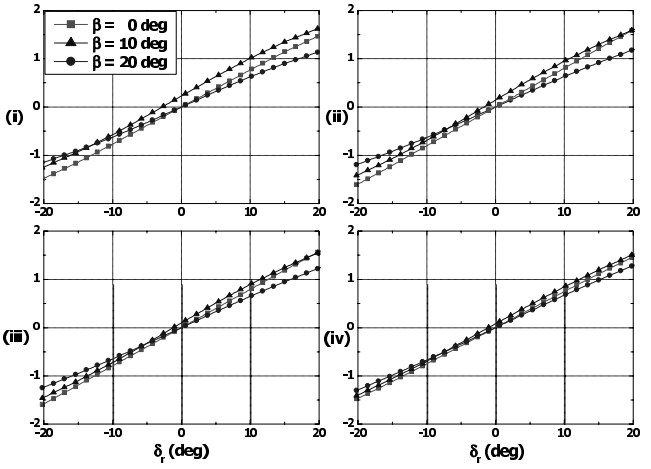

d) C_l versus δ_r with α = 20 deg

Fig. 1 The plot of C_l at (i) $M = 1.5$, (ii) $M = 2.0$, (iii) $M = 2.5$, and (iv) $M = 3.0$.

of longitudinal motions can be represented by the first two columns and rows in Eq. (5). And the lateral motions are described by the last three columns and rows. Thus, the effects of the other coefficients Z_v, Z_p, M_v, M_p, Y_w, L_w, and N_w are neglected in the decoupled design. It can be expected that the performances of the control system designed with the decoupled equations of motions are not representative of those of the actual nonlinear systems. It can be also known by comparing the eigenvalues between coupled and decoupled dynamic systems. The aim of this study is to control this effect, which leads to the fast unstable motions in roll channels and makes the acceleration control problem more difficult.

B. H_∞ Synthesis for the 5-Degree-of-Freedom Missile Dynamics

Requirements to stabilize roll channel and to maintain the desired normal acceleration in the presence of disturbances and sensor noise are formulated as a H_∞ control problem [12]. Figure 2 shows the input multiplicative uncertainty model, where G is the nominal model, W_Δ is a weighting function which indicates the relative model uncertainty over frequency, and Δ represents unmodeled dynamics assumed to be stable and unknown, except for the norm condition $\|\Delta\|_\infty < 1$.

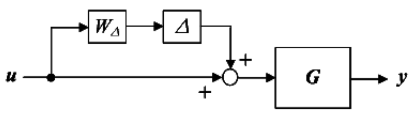

Fig. 2 Multiplicative dynamic uncertainty model.

In this study, the input multiplicative uncertainty weight W_Δ is chosen to be $W_\Delta = w_\Delta(s) I_3$, with a scalar valued function $w_\Delta(s)$:

$$w_\Delta = 50 \frac{s + 100}{s + 10,000} \tag{6}$$

The particular uncertainty weight indicates that at low frequency, there is potentially a 50% modeling error, and at a frequency of 170 rad/s, the uncertainty in the model is up to 100%, and gets larger at higher frequencies.

A block diagram of the closed-loop system is shown in Fig. 3, with reference signal $r_c = [a_z \quad a_y \quad \phi]^T$, measurement noise n, control inputs $u = [\delta_z \quad \delta_r \quad \delta_y]^T$, plant outputs $y_1 = [a_z \quad a_y \quad \phi]^T$, $y_2 = [p \quad q \quad r]^T$, and two weighted outputs z_1 and z_2. The plant G_u is a missile model with input multiplicative uncertainty and K is the controller to be designed. The weights W_i, W_n, and W_r indicating importance and frequency content of set points and noise signals were chosen as $W_i(s) = I_3$, $W_n(s) = 0.001 \times I_3$, and $W_r(s) = I_3$. We only consider measurement noise here, because input disturbances are already included in G_u. The performance weight W_e and control weight W_u reflecting the desired frequency content of the error $(y_1 - r_s)$ and the control signals u were also chosen as

$$W_e(s) = \text{diag}\left[\frac{(s/\sqrt[n]{M_1} + w_1)^n}{(s + w_1\sqrt[n]{A})^n} \times I_2, \frac{(s/\sqrt[n]{M_2} + w_2)^n}{(s + w_2\sqrt[n]{A})^n}\right] \tag{7}$$

$$W_u(s) = 10^{-5} \times I_3 \tag{8}$$

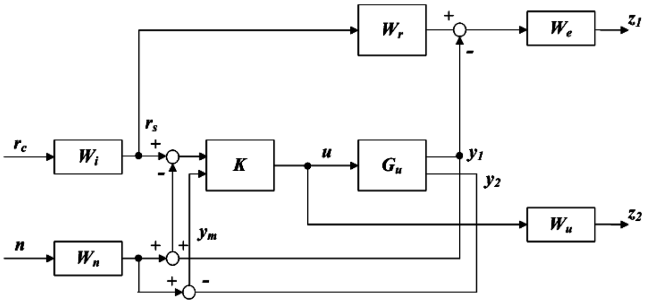

Fig. 3 Interconnection structure for the integrated autopilot.

where $M_1 = 0.15$, $M_2 = 0.5$, $w_1 = 30$, $w_2 = 1$, $A = 10^{-4}$, and $n = 2$. It is essential that the elements of the performance weight W_e be independently endowed with requirements for maneuvering accelerations and an Euler angle. Finding appropriate weighting functions is a crucial step in robust controller design, which usually needs a few trials [13].

MATLAB Robust Control Toolbox is used for controller synthesis. Typical loop shapes can be seen from the singular values of the closed-loop transfer function matrices from the reference command to each of the two outputs, that is, error and output. These two transfer function matrices, which are known as sensitivity function and complementary sensitivity function, are defined as follows:

$$S(s) \triangleq (I + L(s))^{-1} \tag{9}$$

$$T(s) \triangleq L(s)(I + L(s))^{-1} = I - S(s) \tag{10}$$

where loop transfer function matrix $L(s) = G(s)K(s)$. Figure 4 shows the singular value plot of $L(s)$. It shows the good tracking performance in low-frequency range and good robustness and good noise rejection at high-frequency range.

C. Linear Parameter Varying Controller Formulation

To implement the proposed roll–pitch–yaw integrated autopilot, we represent the missile dynamics augmented with the weighting functions using LPV of the following form:

$$\begin{bmatrix} \dot{x} \\ z \\ y \end{bmatrix} = \begin{bmatrix} A(\rho(t)) & B_1(\rho(t)) & B_2(\rho(t)) \\ C_1(\rho(t)) & D_{11}(\rho(t)) & D_{12}(\rho(t)) \\ C_2(\rho(t)) & D_{21}(\rho(t)) & D_{22}(\rho(t)) \end{bmatrix} \begin{bmatrix} x \\ w \\ u \end{bmatrix} \tag{11}$$

where $\rho(t)$ is a scheduling parameter and the signals are x, the state variables, u the control inputs, $y = [\, r_s \quad y_m \,]^T$ the measured outputs, $z = [\, z_1 \quad z_2 \,]^T$ the error, and $w = [\, r_c \quad n \,]^T$ the exogenous signals in the setting of Fig. 3. By assuming the system matrices in Eq. (11) to be affine in ρ, usually, $\rho \in P \subset \Re^m$ where P is a polytope in $\Re^m$, they belong to the polytope S defined by

$$S := Co\left\{ \begin{pmatrix} A_i & B_{1i} & B_{2i} \\ C_{1i} & D_{11i} & D_{12i} \\ C_{2i} & D_{21i} & D_{22i} \end{pmatrix}, i = 1, 2, \ldots \right\} \tag{12}$$

where $A_i, B_{1i}, \ldots, D_{22i}$ denote the values of the matrices $A(\rho), B_1(\rho), \ldots, D_{22}(\rho)$ at the vertices of the parameter polytope P. $Co\{\cdot\}$ indicates the convex hull of a finite number of matrices. It is assumed that the system matrices $B_2(\rho)$, $C_2(\rho)$, $D_{12}(\rho)$, and $D_{21}(\rho)$ are parameter independent, and that, in addition, there is no direct effect from the input to the measurement output, that is, $D_{22}(\rho) = 0$. Following these assumptions, the values of the matrices of the LPV controller can be written as

$$K(\rho) = \sum_{i=1}^{r} \alpha_i K_i = \sum_{i=1}^{r} \alpha_i \begin{pmatrix} A_{Ki} & B_{Ki} \\ C_{Ki} & D_{Ki} \end{pmatrix} \tag{13}$$

where $(\alpha_1, \alpha_2, \ldots, \alpha_r)$ is any solution to the convex decomposition problem

$$\rho = \sum_{i=1}^{r} \alpha_i \rho_i$$

The problem is then to find an LPV controller $K(\rho)$ satisfying Eq. (13) and such that 1) the closed-loop system is stable for all admissible parameter trajectories $\rho(t)$, and 2) the worst-case closed-loop rms gain from w to z does not exceed some level $\gamma > 0$.

Explicit formulas for the controller K_i can be obtained by considering the mapping from exogenous inputs w and control inputs u to controlled outputs z and measured outputs y

$$\begin{bmatrix} z \\ y \end{bmatrix} = P(s) \begin{bmatrix} w \\ u \end{bmatrix} = \begin{bmatrix} P_{11}(s) & P_{12}(s) \\ P_{21}(s) & P_{22}(s) \end{bmatrix} \begin{bmatrix} w \\ u \end{bmatrix} \tag{14}$$

$$u = K(s)y \tag{15}$$

With these formulations, the H_∞ optimal control problem is to find a stabilizing output feedback law $u = K(s)y$ such that the closed-loop transfer function $F_l(P, K)$ from w to z satisfies

$$\|F_l(P, K)\|_\infty < \gamma \tag{16}$$

Given any proper controller $K(s)$ of realization

$$K(s) = D_K + C_K(sI - A_K)^{-1}B_K \tag{17}$$

a realization of the closed-loop transfer function from w to z can be obtained as

$$F_l(P, K) = D_{cl} + C_{cl}(sI - A_{cl})^{-1}B_{cl} \tag{18}$$

where

$$A_{cl} = \begin{bmatrix} A + B_2 D_K C_2 & B_2 C_K \\ B_K C_2 & A_K \end{bmatrix} \qquad B_{cl} = \begin{bmatrix} B_1 + B_2 D_K D_{21} \\ B_K D_{21} \end{bmatrix}$$

$$C_{cl} = [\, C_1 + D_{12} D_K C_2 \quad D_{12} C_K \,] \qquad D_{cl} = [D_{11} + D_{12} D_K D_{21}]$$

Using the bounded real lemma, it can be shown that the conditions for the internal stability and the stabilizing controller Eq. (16) are equivalent to the feasibility of the following linear matrix inequality [14]:

$$\begin{pmatrix} A_{cl}^T X_{cl} + X_{cl} A_{cl} & X_{cl} B_{cl} & C_{cl}^T \\ B_{cl}^T X_{cl} & -\gamma I & D_{cl}^T \\ C_{cl} & D_{cl} & -\gamma I \end{pmatrix} < 0 \tag{19}$$

for some symmetric matrix $X_{cl} > 0$. This synthesis can be reduced to finding two symmetric positive definite matrices R and S such that

$$\begin{pmatrix} \mathcal{N}_R & 0 \\ 0 & I \end{pmatrix}^T \begin{pmatrix} A_i R + R A_i^T & R C_{1i}^T & B_{1i} \\ C_{1i} R & -\gamma I & D_{11i} \\ B_{1i}^T & D_{11i}^T & -\gamma I \end{pmatrix} \begin{pmatrix} \mathcal{N}_R & 0 \\ 0 & I \end{pmatrix} < 0 \tag{20}$$

$$\begin{pmatrix} \mathcal{N}_S & 0 \\ 0 & I \end{pmatrix}^T \begin{pmatrix} A_i S + S A_i^T & R B_{1i}^T & C_{1i} \\ B_{1i} S & -\gamma I & D_{11i} \\ C_{1i}^T & D_{11i}^T & -\gamma I \end{pmatrix} \begin{pmatrix} \mathcal{N}_S & 0 \\ 0 & I \end{pmatrix} < 0 \tag{21}$$

$$\begin{pmatrix} R & I \\ I & S \end{pmatrix} \geq 0 \tag{22}$$

where $\mathcal{N}_R$ and $\mathcal{N}_S$ denote basis of the null space of (B_2^T, D_{12}^T) and (C_2, D_{21}), respectively [8,15,16]. The bounded real lemma matrix X_{cl} can be derived by solving

$$X_{cl} \begin{pmatrix} I & R \\ 0 & M^T \end{pmatrix} = \begin{pmatrix} S & I \\ N^T & 0 \end{pmatrix} \tag{23}$$

Two full-column rank matrices M, N such that $MN^T = I - RS$ can be calculated by singular value decompositon, that is, $U\Sigma V^T =$

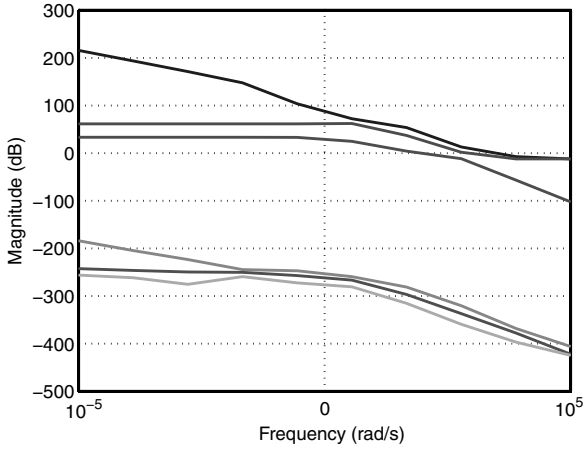

Fig. 4 Singular value plot for loop transfer function $L = GK$.

$I - RS$. Here, U and V are unitary matrices, Σ is a diagonal matrix with nonnegative entries, $M = U\Sigma$, and $N = V$.

V. Simulation Results

In this section, the roll–pitch–yaw integrated controller is tested in nonlinear 5-DOF simulations accounting for cross-coupling effects between the longitudinal and lateral directions. LPV controllers are employed with proportional navigation guidance (PNG) laws optimal for a constant velocity missile [17].

A. Implementation of the Linear Parameter Varying Controller

To test the effectiveness of the LPV controllers in 5-DOF nonlinear setup, two linear time-invariant controllers in Eq. (11) are designed at $M = 2.0$, $a_z = -10g$, $a_y = 10g$, and $M = 2.0$, $a_z = -20g$, $a_y = 20g$, respectively. For various changes in the scheduling variables, which is a total angle of attack in this study, a sequence of acceleration step commands is imposed on the missile trimmed at $M = 2.0$, $a_z = -15g$, and $a_y = 15g$. The initial step command was $a_z = -5g$, $a_y = 5g$, and $\phi = 0$ deg, followed by the second step command of $a_z = 5g$, $a_y = -5g$, and $\phi = 0$ deg. The simulation results under these LPV controllers are shown in Fig. 5. It indicates that the LPV controller provides adequate tracking performance of the guidance commands and smooth coverage of a wider flight envelope rather than only the vicinity of each design point. The roll response was designed to be faster than pitch and yaw channels for stabilization. If the initial roll response is not stabilized fast enough, it can cause difficulty in stabilizing the acceleration channels due to various cross-channel coupling terms that involve the roll rate, such as aerodynamic, control, kinematic, and inertial couplings.

We note that the controller designed based on the decoupled longitudinal and lateral dynamics fails to achieve stable responses against the coupled dynamics. Each of the separate controllers designed based on decoupled longitudinal/lateral dynamics (stated in Sec. IV.A) shows the satisfactory tracking performance against the longitudinal/lateral channel. Figures 6a and 6b show the closed-loop eigenvalue locations and the zoomed-in view, respectively. In those figures, triangles represent the closed-loop eigenvalues of the longitudinal channel only, and circles represent the closed-loop eigenvalues of the lateral channel only. They are all in the open left half-plane. However, when those controllers are combined and

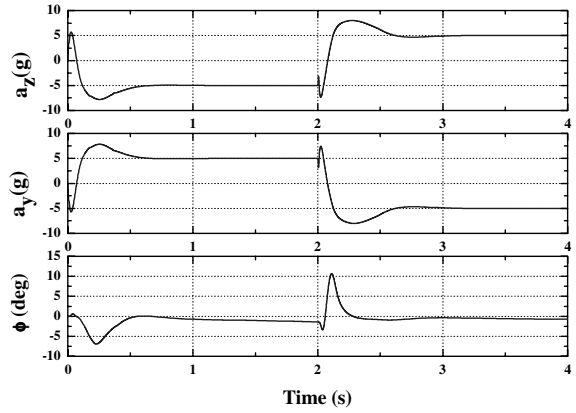

a) Step responses

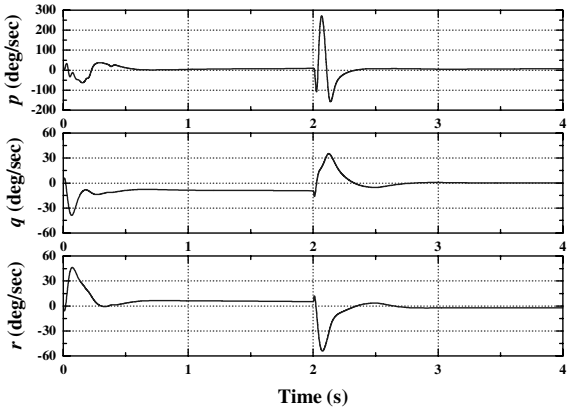

b) State variables

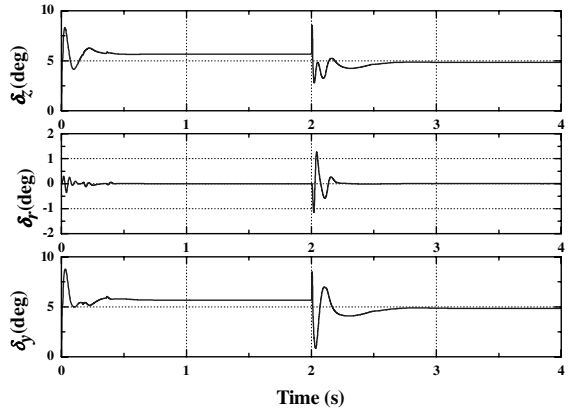

c) Control inputs used

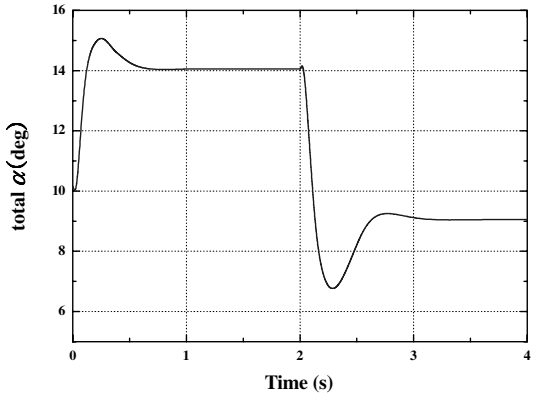

d) Total angle of attack

Fig. 5 Nonlinear 5-DOF simulation results under LPV controllers.

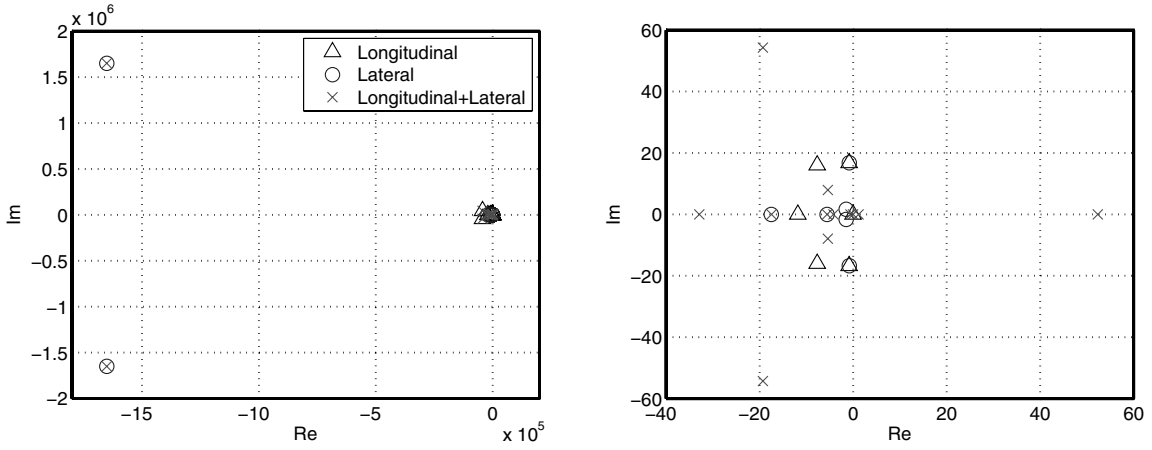

a) Eigenvalue plot **b) Zoomed-in view**

Fig. 6 Eigenvalues for closed-loop system.

applied to the overall coupled dynamics, there are two unstable closed-loop eigenvalues, as shown with crosses in Figs. 6a and 6b.

B. Three-Dimensional Engagement

A three-dimensional pursuit-evasion scenario is engaged to test the proposed autopilot with a PNG law [17]. The missile is initially trimmed at $a_z = -10g$ and $a_y = 10g$ and is assumed to have $\pm 7g$ acceleration limits in longitudinal and lateral motions, respectively. The evader dynamics considered in this study are 3-DOF point-mass model [18]. The target simply performs a $-3g$ pull-up and $3g$ breakaway maneuvers, with the negative sign indicating the upward direction. The initial velocity is set to be 680 m/s, starting from the origin with $\gamma = 0$, and $\psi = 0$ deg. Initial location of the target is (3500,2800,1500), with the velocity 280 m/s and $\gamma = -10$, $\psi = 180$ deg.

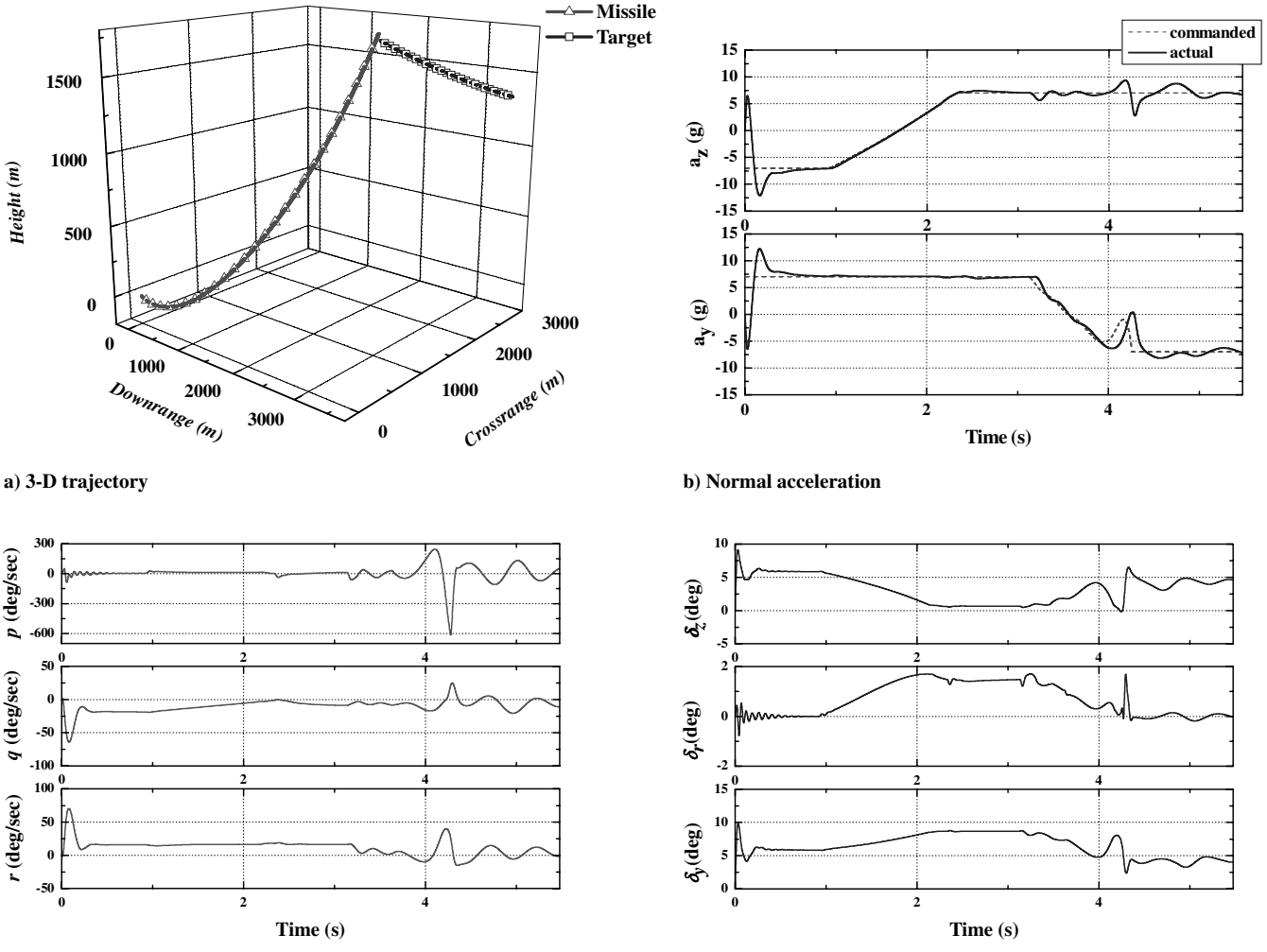

a) 3-D trajectory **b) Normal acceleration**

c) State variables **d) Control inputs used**

Fig. 7 Three-dimensional engagement.

The results of the scenario are shown in Fig. 7. Figure 7a shows three-dimensional trajectories of the missile and target. The longitudinal and lateral acceleration histories and guided commands are also shown in Fig. 7b. As we expected, a slight performance degradation caused by the cross-coupling effects among roll, pitch, and yaw channels at about 4 s is noticeable; it nevertheless indicates that the proposed autopilot exhibits good guidance tracking performance. The state variables and control inputs used in this simulation are shown in Figs. 7c and 7d, respectively. In Fig. 5b, the initial oscillations and large angular rate in a roll channel indicate sensitivity to the rapid changes in guidance commands. Adjusting the weighting functions in the design procedure may suppress both features. However, reducing these effects in the roll channel can slow down the response in other channels. It could then give rise to a reduced agility, resulting in an unpredictable performance degradation.

VI. Conclusions

In this work, following investigations of the aerodynamic characteristics for a surface-to-air missile, which reveal strong cross-coupling effects between the longitudinal and lateral dynamics, we designed roll–pitch–yaw integrated autopilots for the pitch/yaw acceleration and roll angle tracking problem. The proposed autopilot based on the H_∞ control techniques is evaluated in a fully nonlinear 5-DOF simulation. The results showed that the proposed controller performs well in terms of the accurate tracking of the command as well as stabilizing the longitudinal and lateral motions when the nonlinearities and cross-coupling effects dominate the missile dynamics. The designed controllers are scheduled as a function of total angle of attack in the LPV framework to examine the full-envelope control capability. These LPV controllers prove the wide-envelope applicability of integrated autopilots beyond individual design points. Furthermore, the 3-D engagement employing PNG laws shows that the methodology used in this work can be applied to the challenge of the tactical missile autopilots.

Acknowledgments

This research was sponsored in part by the Agency for Defense Development under the Grant ADD-09-01-03-03 and by the Institute of Advanced Aerospace Technology at Seoul National University, Korea.

References

[1] Reichert, R. T., "Dynamic Scheduling of Modern-Robust-Control Autopilot Designs for Missiles," *IEEE Control Systems Magazine*, Vol. 12, No. 5, 1992, pp. 35–42.
doi:10.1109/37.158896

[2] Doyle, J. C., Glover, K., Khargonekar, P. P., and Francis, B. A., "State-Space Solutions to Standard H_2 and H_∞ Control Problems," *IEEE Transactions on Automatic Control*, Vol. 34, No. 8, 1989, pp. 832–846.
doi:10.1109/9.29425

[3] Hiret, A., Duc, G., Friang, J. P., and Farret, D., "Linear-Parameter-Varying/Loop-Shaping H_∞ Synthesis for a Missile Autopilot," *Journal of Guidance, Control, and Dynamics*, Vol. 24, No. 5, 2001, pp. 879–886.
doi:10.2514/2.4821

[4] Lin, C. K., and Wang, S. D., "An Adaptive H_∞ Controller Design for Bank-to-Turn Missiles Using Ridge Gaussian Neural Networks," *IEEE Transactions on Neural Networks*, Vol. 15, No. 6, 2004, pp. 1507–1516.
doi:10.1109/TNN.2004.824418

[5] Buschek, H., "Full Envelope Missile Autopilot Design Using Gain Scheduled Robust Control," *Journal of Guidance, Control, and Dynamics*, Vol. 22, No. 1, 1999, pp. 115–122.
doi:10.2514/2.4357

[6] Voorsluijs, G., and Mulder, J., "Parameter-Dependent Robust Control for a Rotorcraft UAV," AIAA Paper 2005-6407, Aug. 2005.

[7] Sadraey, M., and Colgren, R., "Robust Nonlinear Controller Design for a Complete UAV Mission," AIAA Paper 2006-6687, Aug. 2006.

[8] Apkarian, P., Gahinet, P., and Becker, G., "Self-Scheduled H_∞ Control of Linear Parameter-Varying Systems: A Design Example," *Automatica*, Vol. 31, No. 9, 1995, pp. 1251–1261.
doi:10.1016/0005-1098(95)00038-X

[9] Marcos, A., and Balas, G., "Development of Linear-Parameter-Varying Models for Aircraft," *Journal of Guidance, Control, and Dynamics*, Vol. 27, No. 2, 2004, pp. 218–228.
doi:10.2514/1.9165

[10] Natesan, K., Gu, D., and Postlethwaite, I., "Design of Static H_∞ Linear Parameter Varying Controllers for Unmanned Aircraft," *Journal of Guidance, Control, and Dynamics*, Vol. 30, No. 6, 2007, pp. 1822–1827.
doi:10.2514/1.31283

[11] Jun, B., "A Nonlinear Roll Autopilot Based on 5-DOF Models of Missiles," *Proceedings of the 17th IFAC World Congress*, IFAC, Oxford, U.K., July 2008.
doi:10.3182/20080706-5-KR-1001.1355

[12] Skogestad, S., and Postlethwaite, I., *Multivariable Feedback Control: Analysis and Design*, 2nd ed., Wiley, Hoboken, NJ, 2005.

[13] Gu, D. W., Petkov, P. Hr., and Konstantinov, M. M., *Robust Control Design with MATLAB*, Springer, New York, 2005.

[14] Gahinet, P., "Explicit Controller Formulas for LMI-Based H_∞ Synthesis," *Proceedings of the American Control Conference*, Vol. 3, July 1994, pp. 2396–2400.
doi:10.1109/ACC.1994.734988

[15] Becker, G., and Packard, P., "Robust Performance of Linear Parametrically Varying Systems Using Parametrically Dependent Linear Feedback," *Systems and Control Letters*, Vol. 23, No. 3, 1994, pp. 205–215.
doi:10.1016/0167-6911(94)90006-X

[16] Apkarian, P., and Adams, R. J., "Advanced Gain-Scheduling Techniques for Uncertain Systems," *IEEE Transactions on Control Systems Technology*, Vol. 6, No. 1, 1998, pp. 209–228.
doi:10.1109/87.654874

[17] Jeon, I., Lee, J., and Tahk, M., "Impact-Time-Control Guidance Law for Anti-Ship Missiles," *IEEE Transactions on Control Systems Technology*, Vol. 14, No. 2, 2006, pp. 260–266.
doi:10.1109/TCST.2005.863655

[18] Jung, B., Kim, K., and Kim, Y., "Guidance Law for Evasive Aircraft Maneuvers Using Artificial Intelligence," AIAA Paper 2003-5552, Aug. 2003.